

Cooperative upconversion and optical gain in ion-beam sputter-deposited $\text{Er}_x\text{Y}_{2-x}\text{SiO}_5$ waveguides

Kiseok Suh¹, Minkyung Lee¹, Jee Soo Chang¹, Hansuek Lee³, Namkyoo Park³, Gun Yong Sung⁴ and Jung H. Shin^{1,2*}

¹Department of Physics, KAIST 373-1 Guseong-dong, Yuseong-Gu, Daejeon, Rep. of Korea

²Graduate School of Nanoscience and Technology (WCU), KAIST
373-1 Guseong-dong, Yuseong-Gu, Daejeon, Rep. of Korea

³Optical Communication Systems Laboratory, School of Electrical Engineering and Computer Sciences
Seoul National University, Seoul 151-744, Republic of Korea

⁴Biosensor Research Team, ETRI, Daejeon 305-700, Rep. of Korea

*jhs@kaist.ac.kr

Abstract: Single-phase, polycrystalline $\text{Er}_x\text{Y}_{2-x}\text{SiO}_5$ thin films were deposited by reactive ion-beam sputter deposition and rapid thermal annealing. Due to the crystalline nature, the silicate thin films provide peak Er^{3+} emission cross-section of $0.9 \pm 0.02 \times 10^{-20} \text{ cm}^2$ that is higher than that in silica. Optical gain, with near 60% inversion, is achieved via optical pumping of a single-mode, ridge-type waveguide with the silicate core with an Er concentration of $1.7 \times 10^{20} \text{ cm}^{-3}$. Analysis of pump-power dependence of the optical gain and spontaneous emission intensity of Er^{3+} indicate that the gain is limited by cooperative upconversion process, whose coefficient is determined to be $(8 \pm 3) \times 10^{-17} \text{ cm}^3/\text{sec}$.

©2010 Optical Society of America

OCIS codes: (230.4480) Optical amplifiers; (160.5690) Rare-earth-doped materials.

References and links

1. See, for example, S. Photonics, Topics in Applied Physics (Springer, Berlin, 2004) Vol. 94.
2. A. W. Fang, H. Park, O. Cohen, R. Jones, M. J. Paniccia, and J. E. Bowers, "Electrically pumped hybrid AlGaInAs-silicon evanescent laser," *Opt. Express* **14**(20), 9203–9210 (2006).
3. L. Pavesi, L. Dal Negro, C. Mazzoleni, G. Franzò, and F. Priolo, "Optical gain in silicon nanocrystals," *Nature* **408**(6811), 440–444 (2000).
4. W. J. Miniscalco, "Er-doped glasses for fiber amplifiers at 1500 nm," *J. Lightwave Technol.* **9**(2), 234–250 (1991).
5. A. Polman, D. C. Jacobson, D. J. Eaglesham, R. C. Kistler, and J. M. Poate, "Optical doping of waveguide materials by MeV Er implantation," *J. Appl. Phys.* **70**(7), 3778 (1991).
6. A. Polman, "Erbium implanted thin film photonic materials," *J. Appl. Phys.* **82**(1), 1 (1997).
7. K. Suh, J. H. Shin, S.-J. Seo, and B.-S. Bae, "Large-scale fabrication of single-phase Er_2SiO_5 nanocrystal aggregates using Si nanowires," *Appl. Phys. Lett.* **89**(22), 223102 (2006).
8. M. Miritello, R. Lo Savio, F. Iacona, G. Franzò, A. Irrera, A. M. Piro, C. Bongiorno, and F. Priolo, "Efficient luminescence and energy transfer in erbium silicate thin films," *Adv. Mater.* **19**(12), 1582–1588 (2007).
9. X. J. Wang, T. Nakajima, H. Isshiki, and T. Kimura, "Fabrication and characterization of Er silicates on SiO_2/Si substrates," *Appl. Phys. Lett.* **95**(4), 041906 (2009).
10. K. Suh, and H. J. Shin, S.-J. Seo, and B.-S. Bae, "Er³⁺ luminescence and cooperative upconversion in $\text{Er}_x\text{Y}_{2-x}\text{SiO}_5$ nanocrystal aggregates fabricated using Si nanowires," *Appl. Phys. Lett.* **92**, 121910 (2008).
11. M. P. Hehlen, N. J. Cockroft, T. R. Gosnell, A. J. Bruce, G. Nykolak, and J. Shmlovich, "Uniform upconversion in high-concentration Er^{3+} -doped soda lime silicate and aluminosilicate glasses," *Opt. Lett.* **22**(11), 772–774 (1997).
12. JCPDS powder diffraction file: #52–1809 (Er_2SiO_5), #52–1810 (Y_2SiO_5).
13. D. E. McCumber, "Einstein relations connecting broadband emission and absorption spectra," *Phys. Rev.* **136**(4A), A-954–A-957 (1964).
14. E. Hecht, *Optics* 4th ed. (Addison Wesley, 2002).
15. P. G. Kik, and A. Polman, "Cooperative upconversion as the gain-limiting factor in Er doped miniature Al_2O_3 optical waveguide amplifiers," *J. Appl. Phys.* **93**(9), 5008 (2003).

16. G. N. van den Hoven, E. Snoeks, A. Polman, C. van Dam, J. W. van Uffelen, and M. K. Smit, "Upconversion in Er-implanted Al₂O₃ waveguides," *J. Appl. Phys.* **79**(3), 1258 (1996).
 17. Y. C. Yan, A. J. Faber, H. de Waal, P. G. Kik, and A. Polman, "Erbium-doped phosphate glass waveguide on silicon with 4.1 dB/cm gain at 1.535 μm ," *Appl. Phys. Lett.* **71**(20), 2922 (1997).
 18. R. Lo Savio, M. Mirittello, F. Iacona, A. M. Piro, M. G. Grimaldi, and F. Priolo, "Thermal evolution of Er silicate thin films grown by rf magnetron sputtering," *J. Phys. Condens. Matter* **20**(45), 454218 (2008).
-

1. Introduction

A great interest lies in developing a light source that can be integrated on-chip to power the emergent Si photonics circuits [1]. Of the many approaches that have been explored [2–4], use of Er³⁺ ions has the advantages of proven, stable, and low-noise operation at the technologically important 1.54 μm region. Traditionally, amorphous silica and related materials have been used widely for Er doping [4]. However, silica has refractive index of only 1.44, and the maximum amount of Er that can be doped into silica without inducing optical de-activation is limited to $\sim 1 \times 10^{20} \text{ cm}^{-3}$ only [5,6]. As a consequence the devices tend to be large with low gain, making their use in compact, on-chip integration problematic.

Recently, Er silicates were reported by many researchers as a possible alternative [7–9]. They have refractive indices in the range of 1.7–1.9, and since Er is a major constituent instead of a dopant, can provide optically active Er concentrations that exceed 10^{22} cm^{-3} [8]. However, pure Er silicates are not suitable for 1.54 μm applications as the extremely high Er concentration leads to effects such as concentration quenching [8] and cooperative upconversion [10] that introduce strong non-radiative recombination paths for the 1.54 μm luminescence. Recently, we have reported that by using a chemical solution method to synthesize Er_xY_{2-x}SiO₅ nanocrystal powders from solutions, it is possible to dilute the Er concentration to arbitrary values while maintaining the crystal structure, as Er₂SiO₅ and Y₂SiO₅ have the same crystalline structure and nearly identical lattice constants [10]. More importantly, the cooperative upconversion coefficient (CUC) was found to be only $2.2 \pm 1.1 \times 10^{-18} \text{ cm}^3/\text{s}$ at an Er concentration of $1.2 \times 10^{21} \text{ cm}^{-3}$. This value is much lower than those reported previously for Er-doped thin films [11], thus raising the possibility that optical gain in the excess of 40 dB/cm may be possible using silicates.

However, such wet chemical synthesis methods are incompatible with fabrication of planar optical devices. As the luminescent properties of Er³⁺ can be strongly host-dependent, important parameters such as Er³⁺ absorption/emission cross-sections of Er silicate thin films, CUC, and propagation losses need to be known for Er silicate *thin films*. In this paper, we report on fabrication and characterization of polycrystalline Er_xY_{2-x}SiO₅ thin film waveguides using reactive ion beam sputter deposition method. We find that silicate thin film provides a peak emission cross-section of $0.9 \pm 0.02 \times 10^{-20} \text{ cm}^2$ that is higher than that in silica, albeit over a narrower wavelength range. Optical gain, with near 60% inversion, is achieved via optical pumping of a single-mode, ridge-type waveguide with the silicate core with an Er concentration of $1.7 \times 10^{20} \text{ cm}^{-3}$. The CUC, unfortunately, is as high as $(8 \pm 3) \times 10^{-17} \text{ cm}^3/\text{sec}$, and is the limiting factor against high optical gain of Er silicate thin films.

2. Sample fabrication

Two amorphous, 275 nm thick Er_xY_{2-x}SiO₅ thin films, one with N_{Er} of $1.7 \times 10^{20} \text{ Er cm}^{-3}$ (henceforth referred to as "low-Er" film), and the other with $6.9 \times 10^{20} \text{ Er cm}^{-3}$ (henceforth referred to as "high-Er" film), were deposited on Si wafers with 10 μm thick thermal oxide via reactive ion beam sputtering of a Si target decorated with Er and Y metal chips in Ar/O₂ environment. The composition of the deposited films was confirmed by Rutherford Backscattering Spectroscopy. After deposition, the films were rapid thermal annealed at 1150 °C for 3 min in flowing O₂ environment. Subsequently, a $\sim 175 \text{ nm}$ thick SiO₂ layer was deposited on top, and $\sim 2 \mu\text{m}$ wide SiO₂ strips were defined by photolithography and etching,

thereby forming a strip-loaded waveguide. Finally, the waveguide facets were mechanically polished to lengths L of 9.3 and 9.9 mm for “low-Er” and “high-Er” waveguides, respectively.

For transmission measurements, a tunable laser was used as the signal light source in the wavelength range of 1510~1599. The polarization of the input beam was controlled to be transverse-electric (TE) with a polarization controller. The nominal input power was -19.9 dBm. For optical gain measurements, two laser diodes with center wavelengths of 1472 and 1482 nm were used to pump Er^{3+} ions in both forward and backward directions. The maximum pump power was 160 mW at 1472 nm and 200 mW at 1482 nm. The signal and pump lights were coupled into a lensed fiber made from a Corning SMF28e fiber by a wavelength-division multiplexer (WDM), and then coupled into the waveguide via end-fire method. The transmitted signals were coupled through lensed fiber and observed by an optical spectrum analyzer (OSA). All spectra are calibrated to the fiber-to-fiber response. A schematic description of the transmission / optical gain measurement setup is shown in Fig. 1

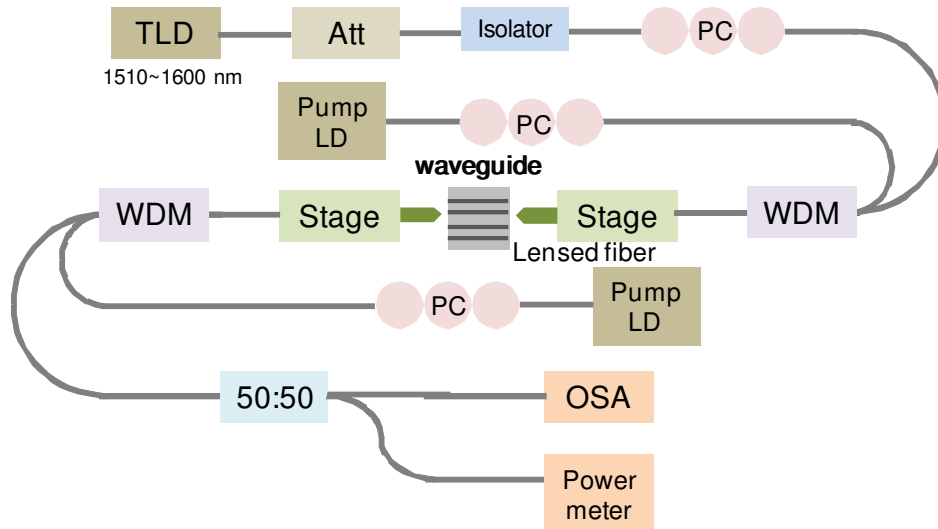


Fig. 1. A schematic description of the transmission / optical gain measurement setup used in the investigation

3. Results and discussion

Figure 2(a) shows typical X-ray diffraction (XRD) spectra of as-deposited and annealed silicate films, together with the expected XRD peak positions of Y_2SiO_5 with a monoclinic symmetry of space group $P2_1/c$, according to the JCPDS cards [12]. We observe emergence of sharp peaks corresponding to Y_2SiO_5 in the XRD spectra after annealing at 1150°C , confirming successful fabrication of single-phase, polycrystalline $\text{Er}_x\text{Y}_{2-x}\text{SiO}_5$. Formation of crystalline phase is reflected in the room temperature photoluminescence (PL) spectrum, as is shown in Fig. 2(b). We observe sharp emission peaks, indicative of crystalline nature of the host, at positions that correspond to those reported for $\text{Er}_x\text{Y}_{2-x}\text{SiO}_5$ nanocrystal powders [10]. Knowing the emission spectrum allows us to calculate the absorption spectrum using the McCumber relationship [13] as well. Note that the absorption cross-section exceeds the emission cross-section in the 1470-1480 nm range. This ensures that population inversion will be possible using the pump laser in this range. On the other hand, as the emission cross-section is not zero within this range, the maximum inversion level will be limited to ~ 0.7 ($1 - \sigma_{\text{emission}}/\sigma_{\text{absorption}}$) due to stimulated emission of Er by the pump beam itself. Figure 2(c) shows the refractive index of annealed film as measured using ellipsometry. By fitting the data to a single-pole Sellmeier equation [14], the refractive index of the film at $1.54\ \mu\text{m}$ is estimated to be 1.67. Finally, Fig. 2(d) shows a scanning electron microscope (SEM) image of the

fabricated “low-Er” waveguide prior to polishing. The silicate layer can be easily discerned by its rough surface due to the polycrystalline structure of the film. Shown in the inset is the calculated TE-mode profile, indicating that the waveguide is single-mode. This will be demonstrated later experimentally. The core-mode overlap Γ is calculated to be 0.4 ± 0.02 . Similar results were obtained for “high-Er” waveguide as well (data not shown).

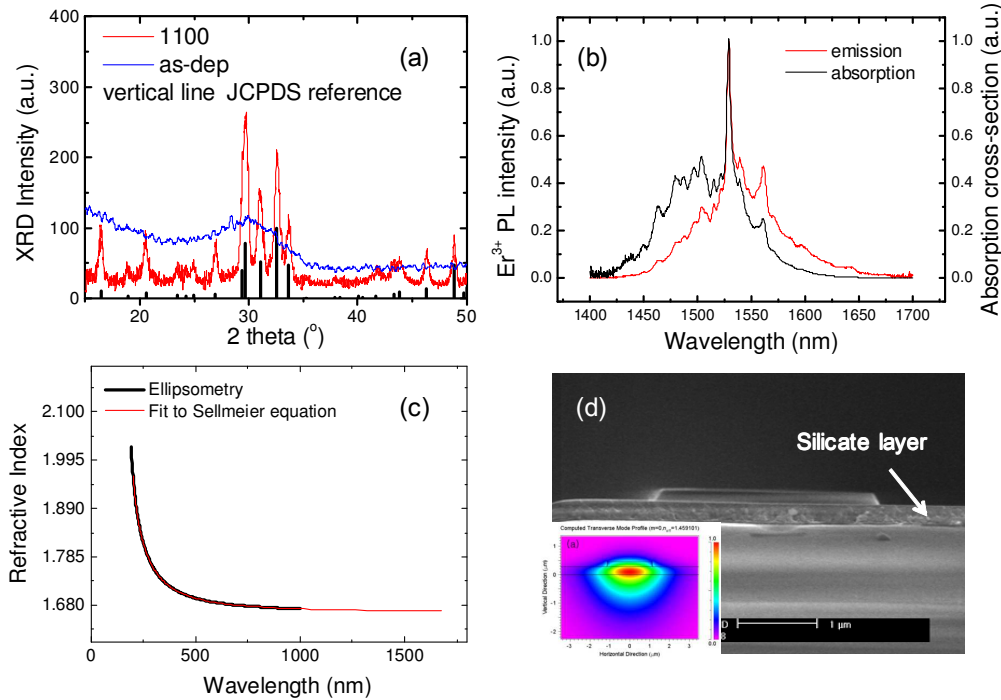


Fig. 2. (a) The X-ray diffraction (XRD) spectra of the as-deposited and annealed films. Also shown are the expected XRD peak positions of Y_2SiO_5 with a monoclinic symmetry of space group $P2_1/c$ according to the JCPDS cards. (b) The room temperature Er^{3+} PL spectrum. Also shown is the absorption spectrum, calculated using the McCumber relationship. (c) Refractive index of the film, as measured by ellipsometry. Also shown is the fit using the single-pole Sellmeier equation. The refractive index at $1.54 \mu m$ is estimated to be 1.67. (d) The SEM image of “low-Er” waveguide prior to polishing. The scale bar represents $1 \mu m$. The inset shows the calculated TE-mode-profile of the waveguide.

Figure 3(a) shows the background-corrected transmission spectrum of the “high-Er” waveguide, together with the calculated Er absorption spectrum. We obtain a near-perfect agreement between the measured and calculated absorption spectra, indicating a high accuracy of the background correction. The maximum Er absorption is found to be 10.8 dB at 1529 nm. Given the Γ of 0.4 and L of 9.9 mm, the maximum Er absorption coefficient σ_{Er} is calculated to be $0.9 \pm 0.02 \times 10^{-20} \text{ cm}^2$ at 1529 nm. This is nearly twice the value of $0.4\text{--}0.8 \times 10^{-20} \text{ cm}^2$ typically used for Er-doped silica fibers [4], and 30% larger than the value of $0.6 \times 10^{-20} \text{ cm}^2$ reported for Er-doped Al_2O_3 [15,16]. We attribute this enhancement to the narrow emission peak of $Er_xY_{2-x}SiO_5$ due to the well-defined lattice sites for Er^{3+} . For amplifier applications, this can present a comparative advantage of silicates over other host materials, as it provides higher optical gain for the same concentration of Er, albeit at the cost of narrower amplification window. Given this value, the “low_Er” waveguide is expected to have

absorption loss of 2.5 dB at 1529 nm ($\text{Er absorption loss} = \Gamma \times \sigma_{\text{Er}} \times N_{\text{Er}} \times L = (0.4) \times (0.9 \times 10^{-20} \text{ cm}^2) \times (1.7 \times 10^{20} \text{ cm}^{-3}) \times (0.93 \text{ cm})$).

Given σ_{Er} , the waveguide coupling and propagation losses were determined by cut-back method, as is shown in Fig. 3(b). Each data point represents the average of at least 9 identically prepared waveguides. Using linear fit, we obtain waveguide coupling and propagation losses of $3.5 \pm 0.2 \text{ dB/facet}$ and $3.4 \pm 0.6 \text{ dB/cm}$, respectively. The measurements were made at 1536 nm; however, we do not expect the loss figures to vary significantly over the range of Er emission.

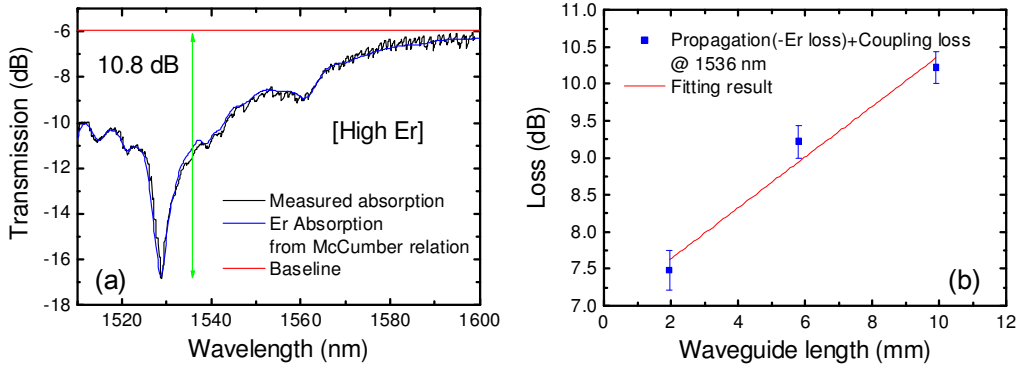


Fig. 3. (a) Base-line corrected transmission spectrum of “high-Er” waveguide. Also shown is the Er absorption spectrum calculated from Er^{3+} photoluminescence spectrum using the McCumber relationship. (b) Waveguide-length dependent transmission loss, obtained by cut-back method at 1536 nm. Each data point represents an average of at least 9 identically prepared waveguides

The gain characteristics of fabricated waveguides are summarized in Figs. 4(a) and 4(b) that show the pump-power dependent signal enhancement of “low-Er” and “high-Er” waveguide at 1529 nm, respectively. Also shown as the inset are the transmission spectra of the waveguides at zero and maximum pump powers. In case of the “low-Er” waveguide, the signal enhancement at 1529 nm is 2.9 dB, which is larger than the Er absorption loss of 2.5 dB expected at that wavelength and indicates an internal optical gain of 0.4 dB. Furthermore, a clear peak in the transmission spectrum is observed at 1529 nm, confirming that population inversion has been achieved. As the signal gain at 1529 nm is given by $\sigma_{\text{Er}}((N_2 - N_1)/N)$, where N_2 is the population in the excited state, N_1 is the population in the ground state, and N is the total Er population, the level of population inversion is estimated to be ~ 0.6 . This is close to the maximum inversion level of ~ 0.7 estimated previously, and indicates that most of the incorporated Er atoms are optically active, in agreement with Ref. [8].

In case of the “high-Er” waveguide, the signal enhancement saturates at a value of 9.8 dB, corresponding to internal optical loss of 1.0 dB. Furthermore, no transmission peak at 1529 nm can be observed, confirming that population inversion did not occur. Based on the internal optical loss of 1.0 dB, the level of population inversion is estimated to be ~ 0.45 .

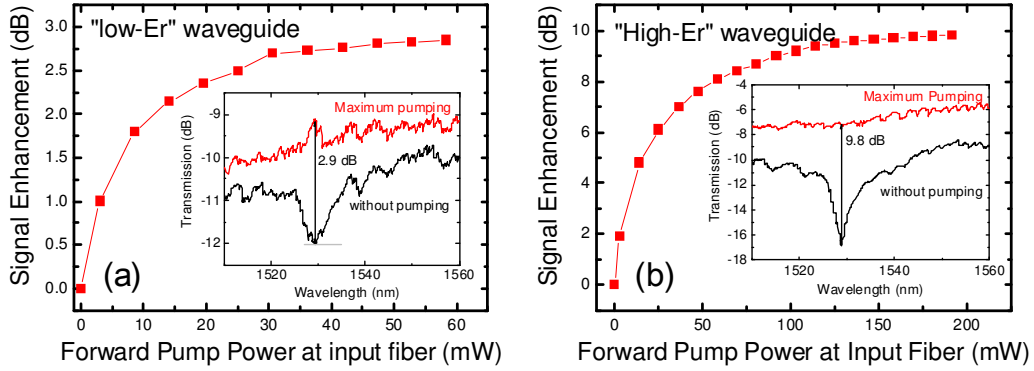


Fig. 4. (a) The gain characteristics of (a) “low-Er” and (b) “high-Er” waveguide at 1529 nm. Also shown as the inset are the transmission spectra of the waveguides at zero and maximum pump powers. Population inversion is achieved for “low-Er” waveguide, but not for the “high-Er” waveguide.

The internal gain of 0.4 dB is much smaller than the waveguide propagation loss of 3.4 dB/cm. Thus, no net gain is achievable in the “low-Er” waveguide. The “high-Er” waveguide could provide net gain, if population inversion were achieved. However, the saturation of signal enhancement from “high-Er” waveguide indicates that no such inversion is possible. This inability to achieve population inversion in “high-Er” sample suggests presence of cooperative upconversion (CU), in which one excited Er^{3+} ion decays non-radiatively by exciting another excited Er^{3+} ion to a higher excited state. As CU increases as the square of population of the excited Er^{3+} ions, it is a dominant process at high Er concentrations [15,16]. In order to investigate the role of CU, the Er^{3+} PL intensities at 981 nm due to ${}^4\text{I}_{11/2} \rightarrow {}^4\text{I}_{15/2}$ (i.e, second-excited to ground state) transition and at 1529 nm to ${}^4\text{I}_{13/2} \rightarrow {}^4\text{I}_{15/2}$ (i.e, first-excited to ground state) transition were obtained from the waveguides during the actual optical gain measurements. As the pump beam itself excites Er into the first excited state only, the PL at 981 nm is purely due to CUC. Figure 5 compares the relative PL intensities at 981 and 1529 nm. In case of the “high-Er” waveguide, the 981 nm PL intensity increases as (1529 nm PL intensity)^{1.78} even at low pump powers, indicating strong CU. The fact that the exponent is 1.78 and not 2 indicates that the CU is so strong that even Er^{3+} ions in the second excited state are being upconverted to even higher excited states. Indeed, as the inset to Fig. 3(a) shows, the “high-Er” waveguide shines bright green even when pumped with 1472 nm, indicating multiple cooperative upconversion. We also note that the green light is straight along the waveguide center, confirming that the waveguides are single-moded around 1530 nm. At pump powers larger than 50 mW, we observe a stronger increase of the 981nm PL intensity that indicates the onset of the excited state absorption (ESA). At this pump power, however, the signal enhancement has already begun to saturate, as can be seen in Fig. 4(b). Thus, Fig. 5, together with Fig. 4, demonstrates that CU is the dominant factor limiting population inversion in “high-Er” $\text{Er}_x\text{Y}_{2-x}\text{SiO}_5$ waveguides.

The 981 nm Er^{3+} PL intensity from the “low-Er” waveguide, on the other hand, does increase as (1529 nm PL intensity)² before ESA becomes dominant above the pump power of 27mW, as shown in Fig. 5(b). Thus, we can neglect the higher order CU in this case, and model the CU process as a 2-level system by fitting the pump power dependence of the 1529 nm Er^{3+} PL intensity to the equation derived for such 2-level CU process [14],

$$I_{Er} \propto \frac{\sigma_{abs}\phi + \sigma_{em}\phi + 1/\tau}{2CN} \left\{ \left[1 + \frac{4CN\sigma_{abs}\phi}{(\sigma_{abs}\phi + \sigma_{em}\phi + 1/\tau)^2} \right]^{1/2} - 1 \right\} \quad (1)$$

where σ_{abs} , σ_{em} , ϕ , τ , C , N is the absorption (excitation) cross section, emission cross section, pump photon flux, Er^{3+} decay lifetime (measured to be 3.36 msec), CUC, and concentration of Er, respectively. As shown in the inset of Fig. 5(b), we obtain a good fit with a CUC value of $(8 \pm 3) \times 10^{-17} \text{ cm}^3/\text{sec}$.

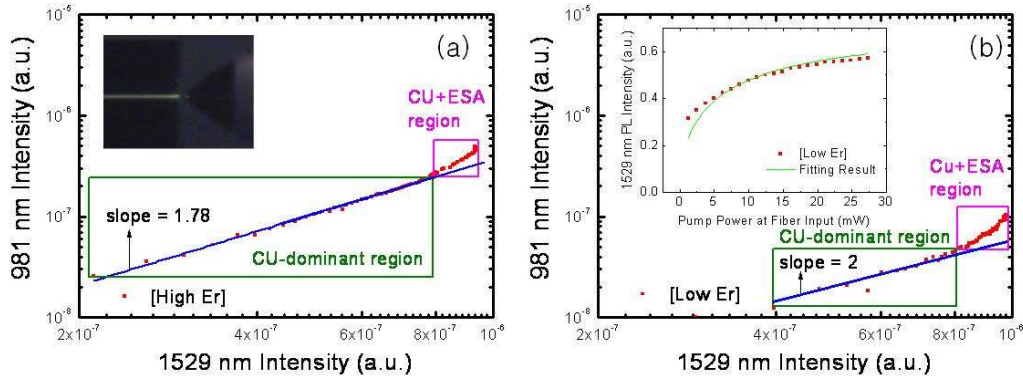


Fig. 5. Comparison of Er^{3+} photoluminescence (PL) intensities, obtained from the waveguides during actual pumping, at 981nm due to ${}^4\text{I}_{11/2} \rightarrow {}^4\text{I}_{15/2}$ (i.e., second-excited to ground state) transition with that at 1529 nm that corresponds to ${}^4\text{I}_{13/2} \rightarrow {}^4\text{I}_{15/2}$ (i.e., first-excited to ground state) transition. Figure 5(a) Shows the results from “high-Er” waveguide. The inset shows an optical microscope image of the waveguide under strong pumping. The green light is due to higher-order cooperative upconversion into the ${}^2\text{H}_{11/2}$ state. Note that the green light, which indicate propagation of the 1480 nm pump beam, is straight, confirming single-mode operation of fabricated waveguides in 1500 nm wavelength range. Figure 5(b) shows the results from the “low-Er” film. The inset shows the results of fitting Eq. (1) to 1531 nm PL intensity, indicating a CUC of $(8 \pm 3) \times 10^{-17} \text{ cm}^3/\text{sec}$

This value of CUC is, unfortunately, nearly 2 orders of magnitude larger than that reported from chemically synthesized nanocrystal $\text{Er}_x\text{Y}_{2-x}\text{SiO}_5$ powder with comparable Er concentration [10]. As CUC tends to increase with increasing Er concentration [11], we can expect the CUC to be even larger for the “high-Er” waveguide. Detailed modeling of the multiple-order CU process in the “high-Er” waveguide is beyond the scope of this paper, but such high value of CUC would be consistent with its inability of “high-Er” sample to achieve population inversion.

On the other hand, we note that the value of $(8 \pm 3) \times 10^{-17} \text{ cm}^3/\text{sec}$ is consistent with the values of CUC reported from other Er-doped thin films – it is even lower than some of them [11,15,16]. Furthermore, it has been reported that bulk glasses always give much lower CUC than the same glasses deposited as a thin film [11]. This indicates that Er silicate structures do not inherently suppress CU, as has been speculated before [9,10]. Rather, the low CUC from $\text{Er}_x\text{Y}_{2-x}\text{SiO}_5$ powder was most likely due to the high crystalline quality of the individual nanocrystals. Thus, short of forming a single-crystalline $\text{Er}_x\text{Y}_{2-x}\text{SiO}_5$ thin film, the extremely low CUC even at very high Er concentrations obtained from $\text{Er}_x\text{Y}_{2-x}\text{SiO}_5$ powders may be difficult to achieve in a thin film. On the other hand, there exist reports that CUC from thin films of the same composition can be reduced by as much as two orders of magnitude, if special care is taken to atomically disperse the Er^{3+} ions [15,17]. Clearly, our method of sputtering Er metal target is not most conducive for uniform, homogeneous dispersal of Er ions, as Er dimers and trimers can be sputtered as well. Therefore, we believe that with better fabrication methods (e.g., ion implantation [15] or RF sputtering of $\text{Er}_x\text{Y}_{2-x}\text{SiO}_5$ targets or

multi-target RF sputtering of Er and Si oxides [8,18]), it should be possible to reduce the CUC from Er silicate thin films to levels that would enable optical gain in excess of 3.5 dB/cm that is necessary to overcome the propagation and coupling losses and to provide net optical gain.

4. Conclusion

In conclusion, we have demonstrated fabrication of single-phase, polycrystalline $\text{Er}_x\text{Y}_{2-x}\text{SiO}_5$ thin film using reactive ion beam sputter deposition followed by rapid thermal anneal. The silicate thin films provide peak emission cross-section of $0.9 \pm 0.02 \times 10^{-20} \text{ cm}^2$ that is larger than that reported from amorphous silica or aluminum oxide based materials, and near full optical activation of the doped Er^{3+} ions. However, the cooperative upconversion process is too strong to obtain optical inversion if the Er concentration is high. Near maximum achievable optical inversion, with internal gain of $\sim 0.5 \text{ dB/cm}$, is achieved when Er concentration is low ($1.7 \times 10^{20} \text{ Er cm}^{-3}$). The cooperative upconversion coefficient in this case was $(8 \pm 3) \times 10^{-17} \text{ cm}^3/\text{sec}$, which is comparable to previously reported values from Er-doped thin films, but is nearly 2 orders of magnitude larger than that reported from chemically synthesized $\text{Er}_x\text{Y}_{2-x}\text{SiO}_5$ nanocrystal powders, indicating that Er silicate structures do not inherently suppress CU. We expect that with better fabrication methods to atomically disperse the Er^{3+} ions, lower values of cooperative upconversion coefficient can be achieved that would enable $\text{Er}_x\text{Y}_{2-x}\text{SiO}_5$ thin films to be used for compact, high-gain optical devices on Si chip.

Acknowledgement

This work was supported in part by OPERA Korea Science and Engineering Foundation (R01-2007-000-21036-0, and KICOS (GRL, K20815000003). J. H. Shin acknowledges support by WCU (World Class University program, grant No.R31-2008-000-10071-0).